Spectroscopic evidence for an engineered, catalytically active Trp radical that creates the unique reactivity of lignin peroxidase

Andrew T. Smith[a,1], Wendy A. Doyle[a], Pierre Dorlet[b], and Anabella Ivancich[b,1]

[b]Centre National de la Recherche Scientifique, Unité de Recherche Associée 2096 and Commissariat à l'Energie Atomique, Institut de Biologie et des Technologies Saclay, Laboratoire des Hyperfréquences, Metalloprotéines et Sytèmes de Spin, F-91191 Gif-sur-Yvette, France; and [a]Department of Chemistry and Biochemistry, School of Life Sciences, University of Sussex, Brighton, BN1 9QG, United Kingdom

Edited by Harry B. Gray, California Institute of Technology, Pasadena, CA, and approved August 12, 2009 (received for review April 27, 2009)

The surface oxidation site (Trp-171) in lignin peroxidase (LiP) required for the reaction with veratryl alcohol a high-redox-potential (1.4 V) substrate, was engineered into *Coprinus cinereus* peroxidase (CiP) by introducing a Trp residue into a heme peroxidase that has similar protein fold but lacks this activity. To create the catalytic activity toward veratryl alcohol in CiP, it was necessary to reproduce the Trp site and its negatively charged microenvironment by means of a triple mutation. The resulting D179W+R258E+R272D variant was characterized by multifrequency EPR spectroscopy. The spectra unequivocally showed that a new Trp radical [*g* values of $g_x = 2.0035(5)$, $g_y = 2.0027(5)$, and $g_z = 2.0022(1)$] was formed after the [Fe(IV)=O Por$^{\bullet+}$] intermediate, as a result of intramolecular electron transfer between Trp-179 and the porphyrin. Also, the EPR characterization crucially showed that [Fe(IV)=O Trp-179$^{\bullet}$] was the reactive intermediate with veratryl alcohol. Accordingly, our work shows that it is necessary to take into account the physicochemical properties of the radical, fine-tuned by the microenvironment, as well as those of the preceding [Fe(IV)=O Por$^{\bullet+}$] intermediate to engineer a catalytically competent Trp site for a given substrate. Manipulation of the microenvironment of the Trp-171 site in LiP allowed the detection by EPR spectroscopy of the Trp-171$^{\bullet}$, for which direct evidence has been missing so far. Our work also highlights the role of Trp residues as tunable redox-active cofactors for enzyme catalysis in the context of peroxidases with a unique reactivity toward recalcitrant substrates that require oxidation potentials not realized at the heme site.

heme peroxidase | high-field EPR spectroscopy | protein engineering | tryptophan radical | electron transfer

The catalytic potential of enzymes is often extended by the presence of key transition metals in the active site, specifically involved in redox reactions. In some cases, amino acid residues can also have a crucial role as redox-active cofactors, in concert with the metal ions (1). The formation of protein-based radicals resulting from the well-controlled oxidation of specific Trp or Tyr residues and the associated intramolecular electron transfer (ET) processes allows the catalytic reaction with substrates having affinity for binding sites removed from the metal active site (2). The oxidation potential of these protein-based radical intermediates could be fine-tuned by the influence of the protein microenvironment without modifications of the usually highly conserved metal active sites (1).

The active site of heme peroxidases consists of a pentacoordinated Fe(III) iron-protoporphyrin IX prosthetic group (Fig. 1), which is capable of one-electron oxidation of substrate(s) binding close to the heme edge. Thus, high valence heme-iron intermediates are responsible for substrate oxidation (3). Fungal peroxidases have been the focus of significant interest due to their possible industrial and environmental applications. Lignin peroxidase (LiP) is one of the fungal enzymes having a key role in the ligninolytic cycle (3); these include manganese peroxidase (MnP), versatile peroxidase (VP), laccase, and H_2O_2-producing enzymes. The ligninolytic cycle is responsible for the degradation of the complex polymer lignin, a key structural component of plant cell walls, whose degradation is rate limiting in the natural carbon cycle. The polymer is insoluble and too large to directly access the very occluded heme active site in LiP (4), where small substrates have been shown to interact (3). Accordingly, it has been proposed that veratryl alcohol (3,4-dimethoxybenzyl alcohol, VA), a secondary metabolite also produced by the fungus during the ligninolytic cycle, could have the role of a diffusible mediator in the reaction with lignin and other large substrates, once oxidized by LiP to the radical form (5). The same mechanism of a diffusible mediator has been proposed for the oxidation of lignin by MnP, except that in this enzyme, a loosely bound Mn^{2+} ion having a binding site close to the heme site is the species reacting with lignin, once oxidized to Mn^{3+} by MnP. Interestingly, an engineering strategy similar to the one described in this work was applied to design MnP activity into a cytochrome *c* peroxidase (CcP) protein scaffold (6–8).

LiP readily oxidizes substrates of redox potentials >1.4 V, possibly requiring VA as mediator (9). Based on structural data (4, 10), and site-directed mutagenesis studies (11), a surface Trp residue (Trp-171) removed from the heme site (Fig. 1), and surrounded by negatively charged residues, was proposed as the oxidation site for VA. The acidic microenvironment of Trp-171 provided by Asp-264, Asp-165, Glu-168, and Glu-250 (the latter being also in H-bonding distance to the indole nitrogen; Fig. 1) could enhance the oxidation potential of the Trp$^{\bullet}$ intermediate, allowing the reaction with VA (1.4 V). However, no direct evidence for the formation of the Trp-171$^{\bullet}$ species or its reactivity with VA has been reported to date, a fact tentatively explained by the short-lived nature of the radical (12). *Coprinus cinereus* peroxidase (CiP) has similar protein fold to LiP, but lacks the VA oxidation activity. We have successfully induced in CiP the capability to oxidize VA by engineering a Trp site that mimics the naturally occurring Trp-171 in LiP (13). In the present work, we have applied EPR spectroscopy as a unique tool to unequivocally characterize the electronic nature of the intermediates formed in the CiP triple variant (D179W+R258E+R272D), containing the engineered Trp site. A new Trp$^{\bullet}$ intermediate was detected in the engineered CiP, and was shown to be the sole reactive species with VA. An engineered MnP is the only previously reported case (14), in which a Trp had been introduced into a homologous position to

Author contributions: A.T.S. and A.I. designed research; A.I. performed research; W.A.D. contributed new reagents/analytic tools; P.D. and A.I. analyzed data; and A.I. and A.T.S. wrote the paper.

The authors declare no conflict of interest.

This article is a PNAS Direct Submission.

[1]To whom correspondence may be addressed. E-mail: a.t.smith@sussex.ac.uk or anabella.ivancich@cea.fr.

This article contains supporting information online at www.pnas.org/cgi/content/full/0904535106/DCSupplemental.

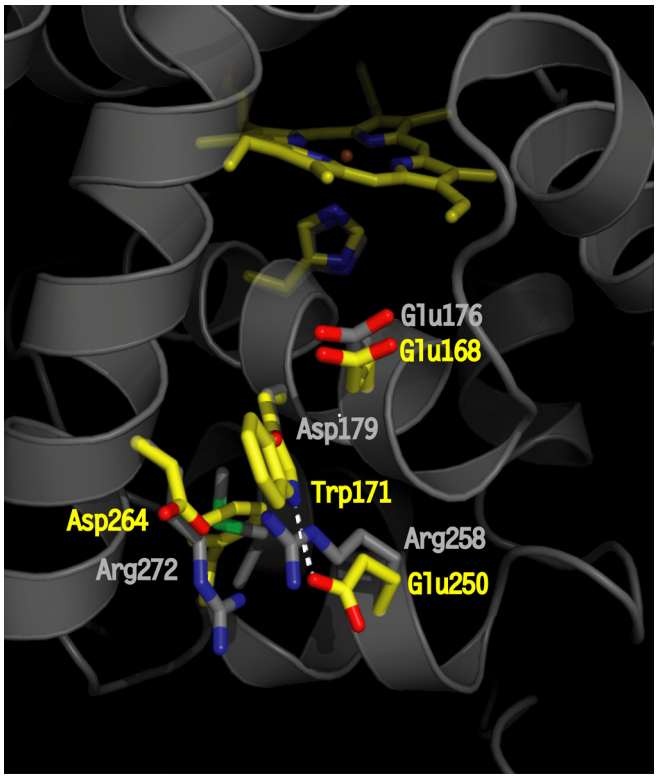

Fig. 1. Crystallographic structure of LiP highlighting the site (residues in yellow) of the catalytically active Trp radical (Trp-171) and its acidic microenvironment (Glu-250, Glu-168, and Asp-264). The residues at homologous positions in WT CiP are shown in gray. The Asp-179 (in CiP) completely overlaps with Trp-171 (in LiP); thus, only the oxygen from the carboxylic group is visible. The figure was prepared by using the coordinates deposited in the Protein Data Bank (accession nos. 1B82 for LiP and 1LYC for CiP).

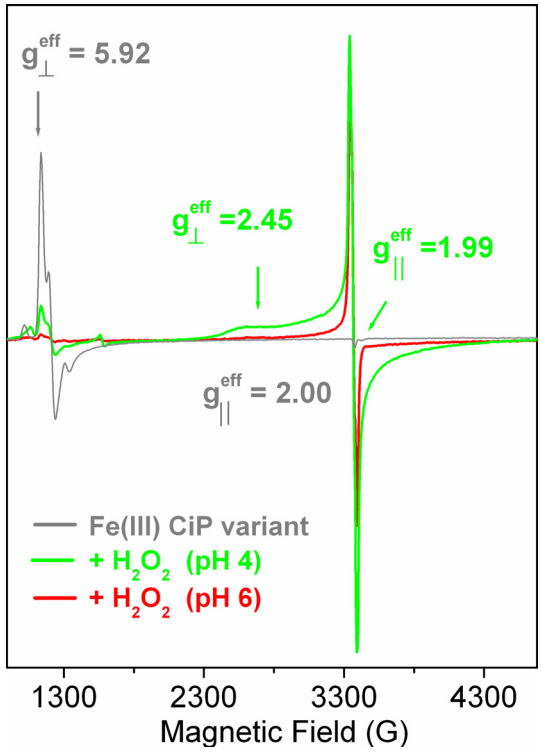

Fig. 2. The 9-GHz EPR spectra of the D179W+R258E+R272D variant of CiP in the resting state (gray trace) and on reaction with hydrogen peroxide (green and red traces). The yield of the very broad and axial spectrum of the [Fe(IV)=O $Por^{\bullet+}$] intermediate was 5 times higher at pH 4.0. The yield of the narrow [Fe(IV)=O $Trp^{\bullet}$] species contributing at $g \approx 2$ was similar at both pHs, indicating a higher conversion to the EPR-silent [Fe(IV)=O] species. Experimental conditions: 4 K; modulation amplitude, 2 G; modulation frequency, 100 kHz.

that of the LiP oxidation site (Trp-171). However, none of the three relevant negatively charged residues that provide the Trp-171 acidic environment (Asp-264, Asp-165, and Glu-250), and which are not conserved in MnP, were included. A low catalytic efficiency for VA oxidation was reported, but no direct evidence for the $Trp^{\bullet}$ formation or its reactivity with VA was given (14).

In the present work, we have used an engineering-based approach that also involved the design and characterization of LiP variants (E250Q, E250Q+E168Q, and E168Q), in which the microenvironment of Trp-171 was modified. The $Trp^{\bullet}$ intermediate was readily stabilized in the E250Q single and double mutations as shown by the EPR $Trp^{\bullet}$ signal, but remained undetected in WT LiP and the E168Q variant. The physicochemical properties related to the radical stabilization, reactivity toward VA, and associated ET process are discussed. This work also highlighted the role of Trp as a tunable redox-active cofactor for enzyme catalysis in the context of peroxidases with a unique reactivity toward substrates that require oxidation potentials not necessarily realized at the metal site. Also, it demonstrates the structural design aspects to be considered to introduce a novel catalytic activity through protein-based radical intermediates, and the required EPR spectroscopy approach to unequivocally assess such a new reactivity.

Results

As shown in Fig. 1, three mutations were necessary to mimic the redox-active Trp site of LiP (residues in yellow) into the CiP enzyme (residues in gray): The substitutions of Asp-179 to introduced the Trp-171 equivalent of LiP, and of two arginines at positions 258 and 272 to provide the H-bond partner to the indole nitrogen, the acidic environment around the Trp, and to make sufficient space to accomodate the new Trp (Fig. 1). This CiP triple variant (D179W+R258E+R272D) was capable of oxidizing VA with a similar pH dependence to LiP (i.e., a maximum at pH 3.5 and drastic drop at pH 6). The k_{cat} was measured to be 12% of the WT LiP enzyme (13). Consequently, the open questions were whether a radical was formed at the engineered Trp-179 site in CiP, and whether this radical was the intermediate reacting with VA. Multifrequency EPR spectroscopy was chosen as a unique tool to determine and discriminate the electronic structures and yields of the metal-radical intermediates formed in the reaction of the CiP variant with hydrogen peroxide, and to identify the intermediate that selectively reacted with the VA substrate.

Characterization of the Radical Intermediates in CiP. Fig. 2 shows the 9-GHz EPR spectra, recorded at 4 K, of the CiP variant in the resting state (gray trace) and after reaction with hydrogen peroxide (green and red traces). The nearly axial signal of the resting enzyme with resonances at $g_{\perp}^{eff} \approx 6$ and $g_{\parallel}^{eff} \approx 2$ (gray trace in Fig. 2) is characteristic of heme iron in the high-spin ferric oxidation state (15). The dramatic decrease in intensity of the ferric signal on reaction with hydrogen peroxide reflected the conversion of the resting enzyme to a high valence intermediate(s) (83 and 95% conversion for pH 4 and 6, respectively). The broad EPR signal (green trace Fig. 2) that appeared concomitantly with the disappearance of the ferric signal, showed spectral features (broadening and temperature-dependent relaxation properties), which were completely consistent with a [Fe(IV)=O $Por^{\bullet+}$] species (16), known as Compound I, the first

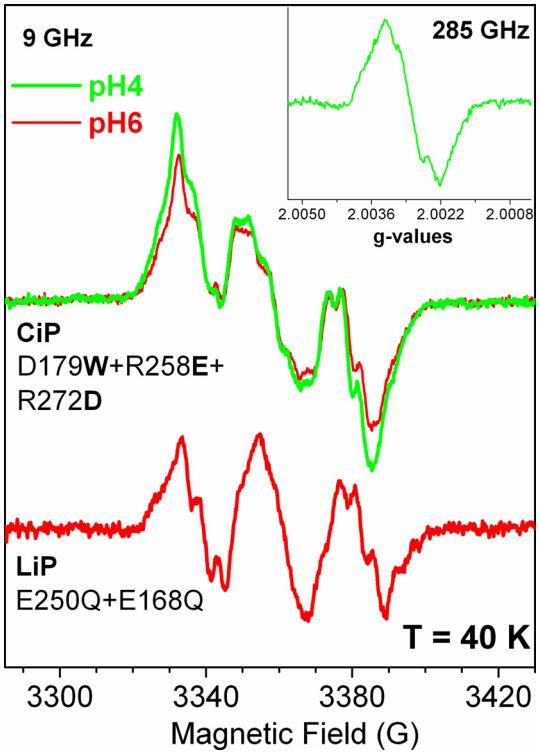

Fig. 3. Conventional (9 GHz, 40 K) and high frequency (285 GHz, 4 K; *Inset*) EPR spectra of the Trp• formed in the CiP triple variant and in the E250Q+E168Q variant of LiP. The 9-GHz EPR spectrum of the Trp is dominated by partially resolved proton hyperfine couplings (Table S1), whereas at higher frequencies, the g values (g_x = 2.0035, g_y = 2.0027, and g_z = 2.0022) were accurately resolved.

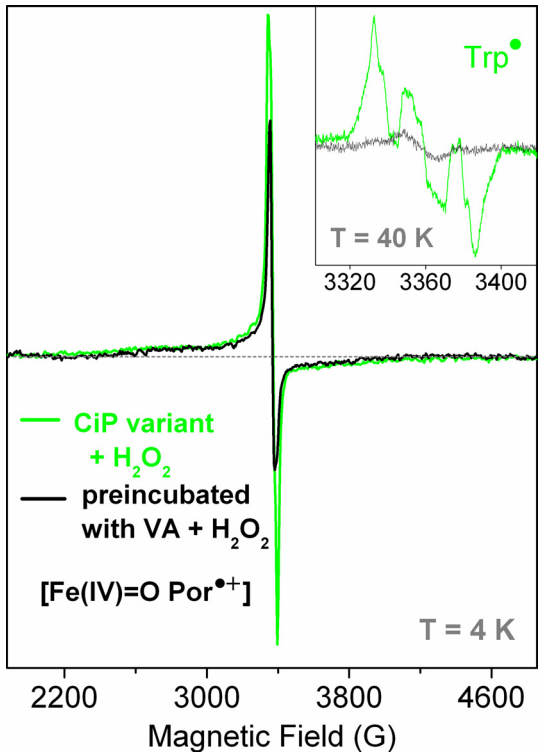

Fig. 4. The reaction of the D179W+R258E+R272D variant of CiP with VA. The enzyme was premixed with 2-fold excess VA before the reaction with hydrogen peroxide (10-s mixing time at 22 °C). The formation of the [Fe(IV)=O Por•+] intermediate (broad and axial EPR signal recorded at 4 K, black trace) was not affected by the presence of VA, but the Trp• signal was clearly absent (black trace; *Inset*).

committed intermediate in the catalytic cycle of peroxidases (3). Specifically, the axial EPR spectrum with effective g values of $g_{\perp}^{\text{eff}}$ = 2.45 and $g_{\parallel}^{\text{eff}}$ = 1.99 readily observed on reaction of the enzyme with hydrogen peroxide at pH 4 and 6 (in lower yield for pH 6) was very similar to the [Fe(IV)=O Por•+] species observed in the equivalent reaction of turnip peroxidase isoforms at pH 4.5 (17). The [Fe(IV)=O Por•+] species should not be detected when recording the EPR spectrum at higher temperatures (T ≥ 30 K) due to the relaxation properties imposed by the magnetic interaction of the porphyrin radical with the heme iron (18). Accordingly, the narrower radical signal readily detected at T = 40 K (Fig. 3 *Upper*) was clear evidence for the contribution of a protein-based radical species to the g ≈ 2 region of the [Fe(IV)=O Por•+] spectrum. A similar situation was previously reported for turnip peroxidase isoenzyme 7 at pH 7.7 (figure 3*A* in ref. 17), where both the porphyrin and tyrosyl radicals contributed to the spectrum. In the CiP variant, the 9-GHz EPR spectrum of the protein-based radical (Fig. 3 *Upper*) with an effective isotropic g value of 2.003 and peak-to-trough width of 54 G could be simulated with proton hyperfine coupling tensors (Fig. S1 and Table S1), which agreed well with those previously reported for Trp radicals (19, 20). The advantageous resolution of the radical g-tensor given by the 285-GHz EPR spectrum (Fig. 3 *Inset*) provided accurate g values of 2.0035(5), 2.0027(5), and 2.0022(1) for g_x, g_y, and g_z, respectively. Thus, the g anisotropy ($\Delta g = |g_x - g_z| = 0.0014$) of the radical was totally consistent with that expected for a Trp• (21). Also, the g_x value was consistent with the presence of a hydrogen-bond interaction to the Trp• (22), most likely donated by the Glu inserted at the position of Arg-258 (Fig. 1).

Thus, we concluded that reaction of the CiP variant with 5-fold excess hydrogen peroxide (10-s mixing time at 20 °C) induced the formation of a [Fe(IV)=O Trp•] species both at pH 4 and 6 (see below), subsequent to the [Fe(IV)=O Por•+] intermediate and resulting from intramolecular ET between the Trp introduced at position 179 and the porphyrin. In contrast, the EPR experiments on the reaction of WT CiP showed that the [Fe(IV)=O Por•+] intermediate was rather short-lived and converted spontaneously to the EPR-silent [Fe(IV)=O] intermediate (Fig. S2). No Trp• was detected in WT CiP, only a very low yield of a clearly different radical species, with peak-to-trough of 16 G (Fig. S3). Spin quantification showed that the yield of the CiP narrow radical was only 10% of that of the Trp• in the CiP variant. Together, our findings clearly showed that the formation of the Trp• intermediate in the CiP triple variant resulted from the engineered Trp site (Fig. 1).

Identification of the Trp• As the Catalytic Intermediate in the Oxidation of VA. EPR spectroscopy is well suited for monitoring the reactivity of intermediates with specific substrates, particularly when protein-based radicals are involved in the peroxidase cycle, because in such cases, the electronic absorption spectrum of the heme completely masks the marker bands for Trp and Tyr (23, 24). The CiP variant was premixed with 2-fold excess VA before reaction with a 5-fold excess of hydrogen peroxide. Comparison of the 9-GHz EPR spectrum obtained in these conditions (black trace in Fig. 4) with the spectrum obtained when no VA was present (green trace in Fig. 4) showed that the narrow signal of the Trp• contributing at g ≈ 2 was missing, whereas the shape and yield of the broad axial signal of the [Fe(IV)=O Por•+] species did not change, as judged from the resonance at $g_{\perp}^{\text{eff}}$ = 2.45. Comparison of the same two spectra recorded at 40 K unambiguously showed the absence of the Trp• signal for the

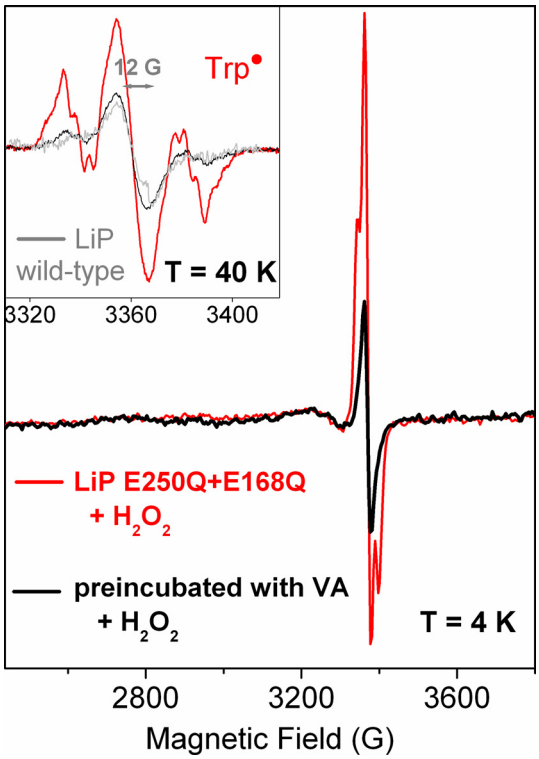

Fig. 5. The 9-GHz EPR spectra of Trp• in the (E250Q+E168Q) variant of LiP (red trace) obtained by the reaction with 5-fold excess H_2O_2 (2-s mixing time at 0 °C). The spectrum of the enzyme premixed with 2-fold excess of VA before the reaction with H_2O_2 showed no Trp• signal. Only a very narrow radical (peak-to-trough of 12 G) was detected (black trace; *Inset*); the same species was already detected in the reaction of the WT LiP with H_2O_2 (gray trace; *Inset*).

sample mixed with VA before the reaction with hydrogen peroxide (Fig. 4 *Inset*). This result provided clear evidence for a catalytically active [Fe(IV)=O Trp-179•] intermediate in the CiP triple variant, and allowed us to confidently rule out the [Fe(IV)=O Por•+] species as the reactive intermediate with VA. Also, the detection of the EPR signal of the [Fe(IV)=O Trp-179•] species at both pH 4 and 6 (Fig. 2), with the H-bond interaction to the indole nitrogen being maintained at pH 6 (as revealed by the 285-GHz EPR spectrum) allowed us to conclude that the drastic drop in the catalytic efficiency of the enzyme with VA at pH 6 is not explained by the absence of the radical, but is most probably a consequence of a pH-induced decrease in the oxidizing potential, which, in turn, makes the reaction with the substrate unfavorable.

Characterization of the Naturally Occurring Tryptophan Radical in LiP Variants. To investigate the physicochemical and structural factors determining the observed differences in kinetic stability of the [Fe(IV)=O Trp•] species in the CiP variant with those occurring in WT LiP, we characterized the three LiP variants, E168Q, E250Q, and E250Q+E168Q, using EPR spectroscopy. The variants were designed to alter the microenvironment of the putative Trp• site of LiP. EPR experiments on the reaction of WT LiP with hydrogen peroxide on ice, expected to slow down the intramolecular ET and possibly detect the Trp• signal showed that the WT LiP converted readily and mostly to the EPR-silent [Fe(IV)=O] species, in agreement with a previous report of similar tests performed at room temperature (25). However, a low yield of a rather narrow organic radical signal (peak-to-trough width of 12 G; gray trace in Fig. 5 *Inset*) was detected. The EPR spectrum of this radical was clearly too narrow to be a Trp• or a Tyr• species, and most probably originates from a thiyl radical (26). It is of importance to note that this narrow radical had been erroneously assigned to the [Fe(IV)=O Por•+] intermediate in a previous report (25). The E168Q variant showed a complete conversion to the EPR-silent [Fe(IV)=O] species within the 2-s reaction time with hydrogen peroxide at 0 °C.

A rather different behavior was observed for the LiP variants in which Glu-250 was replaced by Gln. The EPR spectra of the E250Q and E250Q+E168Q variants clearly showed the formation of a predominant protein-based radical species (red trace in Fig. 5 *Inset*), very similar to the Trp• species in the CiP variant (Fig. 3). The spectra could be simulated with parameters similar to those used for the Trp• species formed in the CiP variant (Fig. S1). It is of note that the extra intensity contributing to the central part of the Trp-171• signal arises from the very narrow radical (peak-to-trough of 12 G) also observed in the WT LiP spectrum (gray trace in Fig. 5 *Inset*). The Trp•-only spectrum resulting from the arithmetic subtraction of the additional radical signal is shown in Fig. 3 (red trace). The Trp• yield in the E250Q+E168Q variant was twice that of the single variant (E250Q), under the same experimental conditions. The E168Q variant had the effect of readily converting the enzyme to the second intermediate (see above). Thus, the higher yield of [Fe(IV)=O Trp•] intermediate in the double mutant could be explained by an additive effect of the single mutations.

To test the reactivity of the Trp-171• with VA, the E250Q+E168Q variant was premixed with VA before the reaction with hydrogen peroxide. In this case, no Trp• signal was detected, in contrast to the experiment without VA present (red trace in Fig. 5). Only the EPR signal of the very narrow radical was detected (black trace in Fig. 5 *Inset*). This result suggests that the [Fe(IV)=O Trp•] species is the reactive intermediate for VA in the LiP variants as demonstrated for the CiP variant. It also constitutes a direct spectroscopic evidence for the radical intermediate previously proposed to be formed on Trp-171 in LiP.

Discussion

For a long time, it has been considered that CcP was the exception among heme peroxidases, because a [Fe(IV)=O Trp•+] species (27) formed subsequently to the short-lived [Fe(IV)=O Por•+] intermediate is responsible for the reaction with the substrate cytochrome *c*. This reaction was shown to require a well-defined ET pathway (28) between the unique radical site, Trp-191, and the binding site for cytochrome *c* on the surface (29). Recent findings on the specific role of tryptophan radicals as oxidizing species in the reaction with substrates in mono and bifunctional peroxidases (19, 20, 23) challenge this view and support the hypothesis that in heme enzymes, specific tryptophan (or tyrosine) residues can either have a role in facilitating ET between redox cofactors (30, 31) or act as true intermediates in the peroxidase cycle (23); thus, generalizing the CcP case.

In LiP, a surface tryptophan has been proposed as an alternative oxidation site for VA. However, no direct evidence in support of the formation of the Trp• has been reported, despite a comprehensive characterization of the enzyme including EPR spectroscopy (25). In this work, we were able to detect the EPR signal of the Trp• in two LiP variants, E250Q and E250Q+E168Q. The replacement of Glu-250 by Gln was chosen to conserve the hydrogen-bond interaction to the indole nitrogen of Trp-171 suggested by the crystal structure of WT LiP while testing the effect of removing the negative charge(s) from the Trp microenvironment (Fig. 1). The formation of the Trp• in the E250Q and E250Q+E168Q variants of LiP agrees well with Gln being an H-bonding partner to Trp-171 in the variants. The higher stability of the Trp• in the variants as compared with the WT LiP could be explained by the decrease in redox potential

of the radical as a result of removing one or more negative charges on the Trp microenvironment, effectively altering the intramolecular ET between Trp-171 and the porphyrin. The ET rates would typically depend on the reduction potential of the Trp$^{\bullet}$, because significant conformational changes that could be rate limiting are not expected as a result of mutations that are largely peripheral to the core fold. It is of note that a large effect in the donor/acceptor ET rates as a function of the Trp reduction potential was predicted in the case of a modified copper protein azurin, in which a Re^{I} complex was tethered to the enzyme surface and a Trp residue was introduced to facilitate ET between the Re^{I} and the distant the Cu^{II} site (figure 4 in ref. 30). In the case of DNA photolyase, a rise in the reduction potential of the enzyme active site induced by the binding of the substrate resulted in an increase (or decrease, depending on pH) in the charge recombination kinetics of $FADH^{-}$ and Trp-306$^{\bullet}$ (32).

The approach of engineering a catalytically active Trp site into a peroxidase, which does not naturally form a Trp$^{\bullet}$ intermediate or react with VA, required the introduction of the Trp residue, as well as its negatively charged microenvironment (residues in gray in Fig. 1). This strategy allowed us to further explore the putative physicochemical properties related to the radical formation as well as the equilibrium between intermediates in relation to intramolecular ET. The characterization by EPR spectroscopy of the CiP triple variant containing the engineered Trp site unequivocally showed that a Trp$^{\bullet}$ species was formed (Fig. 3), in sharp contrast to the WT enzyme (Fig. S2). Also, the EPR signal of the [Fe(IV)=O Por$^{\bullet+}$] intermediate was readily detected in the CiP triple variant (Fig. 2), also in contrast to the WT case (Fig. S2). Relatively small and indirect structural changes on the heme proximal side induced by the mutations, which were suggested by the measurable changes in the ferric EPR signal of the CiP variant (Fig. 2), could explain the different stability of the [Fe(IV)=O Por$^{\bullet+}$] intermediate. A similar situation was previously reported through comparison of turnip peroxidase isoforms (17). Thus, the CiP variant showed long-lived [Fe(IV)=O Por$^{\bullet+}$] and [Fe(IV)=O Trp$^{\bullet}$] intermediates. The distinct EPR spectra of these intermediates allowed us to monitor the reaction with VA and unequivocally identify the Trp$^{\bullet}$ as the reactive species with this substrate, whereas the [Fe(IV)=O Por$^{\bullet+}$] species could be ruled out as intermediate reacting with VA (Fig. 5). Interestingly, the EPR characterization of WT VPs showed a short-lived [Fe(IV)=O Por$^{\bullet+}$] intermediate (thus, not detected even in the millisecond time range) as in WT CiP and LiP, but the Trp$^{\bullet}$ EPR signal was readily detected (20, 33), as in the case of the variants of CiP and LiP (Fig. 3). Comparison of the crystal structures of LiP and *Pleurotus eryngii* VP (34) shows that a methionine residue close by the Trp$^{\bullet}$ site in the VP enzyme is replaced by a phenylalanine (Phe-254) in LiP (unlabeled residue in yellow in Fig. 1). The Met residue close to the Trp$^{\bullet}$ in CcP was proposed to be one of the structural factors stabilizing the radical (35). Similarly, the presence of Met-262 in CiP (unlabeled residue in gray in Fig. 1) could have a role in stabilizing the Trp$^{\bullet}$ in the engineered enzyme. It is tempting to correlate the presence of the Met residue, a more stable Trp$^{\bullet}$ and the lower turnover (and apparent affinity) for VA in the CiP variant and VPs as compared with the LiP case. Kinetic studies on VPs showed that the reaction rate with VA is doubled when the Met is replaced by Phe (M247F) (36). Further studies are planned to disentangle the effect of negative charges in the microenvironment of the Trp$^{\bullet}$ site as well as the relative stability of the intermediates (thus, redox potentials) possibly using a Re^{I} complex tethered to the surface of the enzyme (22, 30). The possibility of generating higher valence intermediates without using H_2O_2 is a valuable tool to better understand the reactivity of the Trp$^{\bullet}$ intermediate toward the substrate VA and its relationship to the preceding [Fe(IV)=O Por$^{\bullet+}$] intermediate and associated charge recombination.

In conclusion, our work shows that, to engineer a catalytically competent Trp site for a given substrate, it is necessary to take into account the physicochemical properties of both the radical and the preceding [Fe(IV)=O Por$^{\bullet+}$] intermediate, the latter formed by intramolecular ET. Our findings on the modification of kinetic stability of the engineered Trp$^{\bullet}$ in CiP induced by the mutations and the equivalent effect obtained with the reverse mutations on the LiP enzyme allowed us to understand better the differences observed between LiP and the *Bjerkandera adusta* and *Pleurotus eryngii* VPs. This work highlights the role of Trp as a tunable redox-active cofactor for enzyme catalysis in the context of peroxidases with a unique reactivity toward recalcitrant substrates that require oxidation potentials not attainable by the heme cofactor. Also, this work opens the possibility of combining the engineered Trp$^{\bullet}$ site with a Re^{I} complex tethered to the surface of the enzyme as a promising system for characterizing issues related to ET in biology, such as superexchange pathways and the role of Trp and Tyr in facilitating electron transport between cofactors or cofactors and substrates.

Materials and Methods

Sample Preparation. Synthesis of the CiP gene, site-directed mutagenesis, preparation of protein extracts from *Escherichia coli* inclusion bodies, protein purification, and activity assays were previously described (13). Recombinant LiPH8 and the variants were expressed in *E. coli* and activated by in vitro refolding of inclusion body material, as described (11). VA (Sigma) was double glass distilled and stored at −80 °C.

Multifrequency EPR Spectroscopy. Conventional 9-GHz EPR measurements were performed by using a Bruker ER 300 spectrometer with a standard TE_{102} cavity equipped with a liquid helium cryostat (Oxford) and a microwave frequency counter (Hewlett Packard 5350B). The home-built high-field EPR spectrometer (95–285 GHz) has been described previously (37). The absolute error in g values was 1×10^{-4}. The relative error in g values between any two points of a given spectrum was 5×10^{-5}.

EPR Samples Preparation. The reaction of resting (ferric) CiP and LiP enzymes was done by mixing manually 40 μL of enzyme in 20 mM succinate buffer, pH 6.0 (or pH 4.0) with an equal volume of 5-fold excess hydrogen peroxide solution (at the same enzyme pH) directly in the 4 mm-EPR tubes kept at 20 °C for the CiP variant or on ice (0 °C) for LiP enzymes (WT and variants). The reaction time was 10 s for CiP and 2 s for LiP. The mixing time and temperature conditions were those providing the maximum yield of Trp$^{\bullet}$ signals for each enzyme. The choice of pH 4 and 6 for characterizing the intermediates formed on reaction of CiP and LiP with H_2O_2 was based on the sharp pH dependency of the VA specific activity of the enzymes, with the maximum turnover measured at pH 3–4 and a drastic decrease at pH 6. For the 9-GHz EPR experiments with the LiP enzymes, an initial concentration of 0.4 mM was used. A high initial enzyme concentration of 1.5 mM was used to obtain well resolved high-field EPR spectra of the Trp radical in the CiP variant; the same samples were tested in the 9-GHz EPR spectrometer.

ACKNOWLEDGMENTS. We thank Sun Un (Commissariat à l'Energie Atomique Saclay) for insights and discussions on HF-EPR spectroscopy and Klaus Piontek (Freibourg) for helpful discussions. A.I. and P.D. were supported by the French Centre National de la Recherche Scientifique and Commissariat à l'Energie Atomique Saclay. A.S. was supported by grants from European Union Fifth Framework Programme BIORENEW and the Biotechnology and Biological Sciences Research Council.

1. Stubbe J, van der Donk W (1998) Protein radicals in enzyme catalysis. *Chem Rev* 98:705–762.
2. Seyedsayamdost MR, Yee CS, Reece SY, Nocera DG, Stubbe J (2006) pH rate profiles of F_nY_{356}-R2s (n = 2, 3, 4) in *Escherichia coli* ribonucleotide reductase: Evidence that Y_{356} is a redox-active amino acid along the radical propagation pathway. *J Am Chem Soc* 128:1562–1568.
3. Dunford B (1999) *Heme Peroxidases* (Wiley, New York), pp 281–308.
4. Choinowski T, Blodig W, Winterhalter KH, Piontek K (1999) The crystal structure of lignin peroxidase at 1.70 Å resolution reveals a hydroxyl group on the Cβ of tryptophan 171: A novel radical site formed during the redox cycle. *J Mol Biol* 286:809–827.
5. Harvey PJ, Schoemaker HE, Palmer JM (1986) Veratryl alcohol as a mediator and the role of radical cation in lignin biodegradation by *Phanerochaete chrysosporium*. *FEBS Lett* 195:242–246.

6. Yeung BKS, Wang X., Sigman JA, Petilo PA, Lu Y (1997) Construction and characterization of a manganese-binding site in cytochrome c peroxidase: Towards a novel manganese peroxidase. *Curr Biol* 4:215–221.
7. Wilcox SK, et al. (1998) Rational design of a functional metalloenzyme: Introduction of a site for manganese binding and oxidation into a heme peroxidase. *Biochemistry* 37:16853–16862.
8. Gengeback A, Syn S, Wang X, Lu Y (1999) Redesign of cytochrome c peroxidase into a manganese peroxidase: Role of tryptophans in peroxidase activity. *Biochemistry* 38:11425–11432.
9. Pasti-Grigsby MB, Paszczynski A, Goszczynski S, Crawford DL, Crawford RL (1992) Influence of aromatic substitution patterns on azo dye degradability by *Streptomyces* spp. and *Phanerochaete chrysosporium*. *Appl Environ Microbiol* 58:3605–3613.
10. Blodig W, Smith AT, Doyle WA, Piontek K (2001) Crystal structures of pristine and oxidatively processed lignin peroxidase and the W171F mutant that eliminates the redox active tryptophan 171. Implications for the reaction mechanism. *J Mol Biol* 305:851–861.
11. Doyle WA, Blodig W, Veitch NC, Piontek K, Smith AT (1998) Two substrate interaction sites in lignin peroxidase revealed by site-directed mutagenesis. *Biochemistry* 37:15097–15105.
12. Blodig W, Smith AT, Winterhalter K, Piontek K (1999) Evidence from spin-trapping for a transient radical on tryptophan residue 171 of lignin peroxidase. *Arch Biochem Biophys* 370:88–92.
13. Smith AT, Doyle WA (2006) Engineered peroxidases with veratryl alcohol oxidase activity, International Patent WO/2006/114616, PCT/GB2006/001515.
14. Timofeevski SL, Nie G, Reading NS, Aust SD (2000) Substrate specificity of lignin peroxidase and a S168W variant of manganese peroxidase. *Arch Biochem Biophys* 373:147–153.
15. Palmer (1983) *Iron Porphyrins*, *Part II*, eds Lever ABP, Gray HB (Addison-Wesley, Reading, MA), pp 43–88.
16. Schulz CE, et al. (1979) Horseradish peroxidase compound I: Evidence for spin coupling between the heme iron and a 'free radical.' *FEBS Lett* 103:102–105.
17. Ivancich A, Mazza G, Desbois A (2001) Comparative Electron Paramagnetic Resonance study of radical intermediates in turnip peroxidase isozymes. *Biochemistry* 40:6860–6866.
18. Colvin JT, Rutter R, Stapleton HJ, Hager LP (1983) Zero-field splitting of Fe^{3+} in horseradish peroxidase and of Fe^{3+} in horseradish peroxidase compound I from electron spin data. *Biophys J* 41:105–108.
19. Pöstch S, et al. (1999) The iron-oxygen reconstitution reaction in Protein R2-Tyr-177 mutants of mouse ribonucleotide reductase. *J Biol Chem* 274:17696–17704.
20. Pogni R, et al. (2005) Tryptophan-based radical in the catalytic mechanism of versatile peroxidase from *Bjerkandera adusta*. *Biochemistry* 44:4267–4274.
21. Un S (2005) The **g**-values and hyperfine coupling of amino acid radicals in proteins: Comparison of experimental measurements with *ab initio* calculations. *Magn Reson Chem* 43:S229–S236.
22. Miller JE, et al. (2003) Spectroscopy and reactivity of a photogenerated tryptophan radical in a structurally defined protein environment. *J Am Chem Soc* 125:14220–14221.
23. Singh R, Switala J, Loewen PC, Ivancich A (2007) Two [Fe(IV)=O Trp•] intermediates in *M. tuberculosis* catalase-peroxidase discriminated by multifrequency (9–285 GHz) EPR spectroscopy: Reactivity toward isoniazid. *J Am Chem Soc* 129:15954–15963.
24. Fielding AJ, et al. (2008) Intramolecular electron transfer versus substrate oxidation in lactoperoxidase: Investigation of radical intermediates by stopped-flow absorption spectrophotometry and (9–285 GHz) electron paramagnetic resonance spectroscopy. *Biochemistry* 47:9781–9792.
25. Khindaria A, Aust SD (1996) EPR detection and characterization of lignin peroxidase porphyrin π-cation radical. *Biochemistry* 35:13107–13111.
26. Balagopalakrishna C, et al. (1998) Superoxide produced in the heme pocket of the β-chain of hemoglobin reacts with the β-93 cysteine to produce a thiyl radical. *Biochemistry* 37:13194–13202.
27. Sivaraja M, Goodin DB, Smith M, Hoffman BM (1989) Identification by ENDOR of Trp191 as the free-radical site in cytochrome c peroxidase compound ES. *Science* 245:738–740.
28. Hays Putnam A-MA, Lee Y-T, Goodin DB (2009) Replacement of an electron transfer pathway in cytochrome *c* peroxidase with a surrogate peptide. *Biochemistry* 48:1–3.
29. Pelletier H, Kraut J (1992) Crystal structure of a complex between electron transfer partners, cytochrome *c* peroxidase and cytochrome *c*. *Science* 258:1748–1755.
30. Shih C, et al. (2008) Tryptophan-accelerated electron flow through proteins. *Science* 320:1760–1762.
31. Colin J, Wiseman B, Switala J, Loewen PC, Ivancich A (2009) Distinct role of specific tryptophans in facilitating electron transfer or as [Fe(IV)=O Trp•] intermediates in the peroxidase reaction of *Bulkholderia pseudomallei* catalase-peroxidase: A multifrequency EPR spectroscopy investigation. *J Am Chem Soc* 131:8557–8563.
32. Kapetanaki SM, Ramsey M, Gindt YM, Schelvis JPM (2004) Substrate electric dipole moment exerts a pH-dependent effect on electron transfer in *Escherichia coli* photolyase. *J Am Chem Soc* 126:6214–6215.
33. Pogni R, et al. (2006) A Tryptophan neutral radical in the oxidized state of versatile peroxidase from *Pleurotus eryngii*. *J Biol Chem* 281:9517–9526.
34. Perez-Boada M, et al. (2005) Versatile peroxidase oxidation of high redox potential aromatic compounds: Site-directed mutagenesis, spectroscopic and crystallographic investigation of three long-range electron transfer pathways. *J Mol Biol* 354:385–402.
35. Jensen GM, Bunte SW, Warshel A, Goodin DB (1998) Energetics of cation radical formation at the proximal active site tryptophan of cytochrome *c* peroxidase and ascorbate peroxidase. *J Phys Chem* 102:8221–8228.
36. Ruiz-Dueñas FJ, et al. (2009) Protein radicals in fungal versatile peroxidase: Catalytic tryptophan radical in both compound I and compound II and studies on W164Y, W164H, and W164S variants. *J Mol Biol* 284:7986–7994.
37. Un S, Dorlet P, Rutherford AW (2001) A high field EPR tour of radicals in photosystems I and II. *Appl Magn Reson* 21:341–361.